DOI:10.1021/jf102005z

JOURNAL OF AGRICULTURAL AND FOOD CHEMISTRY
ARTICLE

Resveratrol and Its Oligomers from Wine Grapes Are Selective $^1O_2$ Quenchers: Mechanistic Implication by High-Performance Liquid Chromatography−Electrospray Ionization−Tandem Mass Spectrometry and Theoretical Calculation

Li-Yan Jiang, Shan He, Ke-Zhi Jiang, Cui-Rong Sun, and Yuan-Jiang Pan*

Department of Chemistry, Zhejiang University, Hangzhou 310027, China

Resveratrol and its oligomers, abundantly present in wine grapes, are believed to be effective phytoalexins for the phenomenon "French paradox" partially by virtue of their powerful antiradical properties. EPR spin-trapping technique was utilized, demonstrating all polyphenols were selective $^1O_2$ quenchers but not effective $^{\bullet}OH$ and $O_2^{\bullet-}$ scavengers. On the basis of the HPLC-ESI-MS^2 analysis for the simulated reactions of polyphenols with $^1O_2$, the molecular weights of the resulting photochemical products were 14 or 28 Da higher than those of their substrates. No fragment C_2H_2O (42 Da), which was rather distinctive of the resorcinol rings in these cases, had been observed, whereas their MS/MS spectra displayed characteristic neutral fragments including carbon monoxide (CO, 28 Da) and 2-hydroxy[1,4]benzoquinone ($C_6H_4O_3$, 124 Da). Finally, PM3 semiempirical calculations and HR-FTICR-MS experiments were performed, supporting the assertion that their quenching mechanism involved physical and chemical pathways. Chemical quenching underwent an endoperoxide intermediate form to generate quinones.

KEYWORDS: Reactive oxygen species; resveratrol; singlet oxygen quenchers; high-performance liquid chromatography−electrospray ionization−tandem mass spectrometry; electron paramagnetic resonance spin-trapping; parametrized method 3 semiempirical calculations

INTRODUCTION

Excess reactive oxygen species (ROS), which are the results of the disturbance in the equilibrium status of prooxidant/antioxidant reactions in living cells, induce oxidative stress to inhibit normal functions of cellular components and then cause serious diseases. Singlet oxygen $^1O_2$, a classical form of ROS, is the first excited state $^1\Delta_g$ of molecular oxygen. Its generation is achieved by not only photosensitized oxidations in aerobic environments (*1*) but also a large number of other biologically relevant processes without light (*2*). Due to the existence of both electrons in the same molecular orbit with paired spins, $^1O_2$ is stable with a long lifetime as $10^{-6}-10^{-5}$ s in biological systems and a calculated energy of only 94 kJ mol^{-1} above the ground state, namely, molecular oxygen (triplet) (*3*). In the presence of some biomacromolecules such as DNA, RNA, proteins, and lipids, $^1O_2$ could undergo kinds of rapid reactions (*4*, *5*). Other excited states of molecular oxygen (e.g., the $^1\Sigma_g$ state that has two highest energy electrons in different orbits with paired spins) are also originated, but they are of higher energy, short-lived as a consequence, and usually undergo rapid spontaneous decay rather than chemical reactions (*3*). Thus, $^1O_2$ is the most highly reactive and dangerous state of molecular oxygen. Previous papers have indicated that $^1O_2$ is generally associated with porphyries, erythropoietic protoporphyria, pellagra (*6*), cataractogenesis (*7*), cancer, and aging (*8*).

*Author to whom correspondence should be addressed (phone +86 571 87953000; fax +86 571 87951629; e-mail panyuanjiang@zju.edu.cn).

Resveratrol and its oligomers are biologically active secondary metabolites mainly found in Vitaceaeous, Dipterocarpaceaeous, Leguminosaeous, Cyperaceaeous, and Gnetaceaeous plants, especially the species of *Vitis vinifera*, the so-called wine grapes. For example, 0.9−3.8 mg L^{-1} resveratrol was determined in 19 French red wines (*9*), and in 14 Madeira wines, it was observed to be 0.77−15.45 mg L^{-1} (*10*). To date, it is conceivable that resveratrol plays a vital role as a prominent phytoestrogen in cancer chemoprevention (*11*, *12*) and cardiovascular modulating effects (*13*, *14*). Increasingly intense research has been devoted to its antiradical (ROS) activity in recent years (*15*) as well as its oligomers and their chemical structures (**Figure 1**). On the basis of the proposed free radical mechanism, a diverse assemblage of resveratrol radicals caused by certain peroxidases could lead to the formation of oligomers with a single structural feature. These oligomers have significant potential in treating diseases because of their antioxidant, anti-inflammatory, anti-HIV, antitumor, hepatoprotective, and cycoloxygenase inhibitory activities (*16*). In essence, the performance of oligomers' multiple activities could be traced back to their inhibitory effects on ROS involving $^1O_2$. In our previous work (*17*), pallidol (**Figure 1**), a resveratrol dimer reported to be present at levels (0.5−4.8 mg L^{-1}) equivalent to those of resveratrol in 19 French red wines (*9*), has been isolated and exhibited a selective quenching effect on $^1O_2$, whereas no potent scavenging activities on hydroxyl radical $^{\bullet}OH$ and superoxide anion $O_2^{\bullet}$ had been shown. It is interesting that the same phenomena have also been observed for two

 Published on Web 08/02/2010

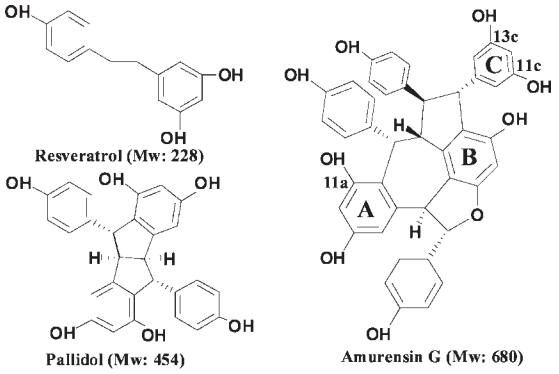

Figure 1. Chemical structures of resveratrol (monomer), pallidol (dimer), and amurensin G (trimer).

resveratrol tetramers (*18*) and one hexamer (*19*). All of these observations prompted us to further investigate the quenching mechanism of resveratrol and its oligomers on $^1O_2$.

To the best of our knowledge, high-performance liquid chromatography−electrospray ionization−tandem mass spectrometry (HPLC-ESI-MS^2) is sensitive, rapid, convenient and provides considerable structural information. Generally speaking, compared to the blank control reaction systems where no reaction happens because the absence of some indispensable conditions such as photosensitizers, some thoroughly separated peaks appear and are analyzed by ESI-MS^2 to give molecular weights and characteristic fragments or ions. Then the chemical structures could be deduced from the reactant/substrate and confirmed by the analysis of elemental composition with HR-FTICR-MS experiments. Thus, the mechanism, even for unstable products/intermediates, can be figured out. So far, the technique has been successfully applied for some systematic mechanistic research (*20*, *21*). Furthermore, up to now, theoretical calculations as assistant tools have been generally carried out to model the possible transition states and further determine the potential reaction pathways by the evaluation of Gibbs free energies, especially for some free radical related reactions due to their unstable properties (*22*−*24*). Parametrized method 3 (PM3) semiempirical calculations are recognized as one of the most accurate semiempirical approaches for computing purposes, and the presence of only one negative frequency confirms the existence of real transition states.

In this study, EPR results highlighted that resveratrol, pallidol, and amurensin G from wine grapes, the structures of which are shown in **Figure 1**, were selective on quenching $^1O_2$ but not rather effective on scavenging $^{\bullet}OH$ and $O_2^{\bullet}$. We aimed at making the associated mechanism clear, using HPLC-ESI-MS^2 technique in combination with PM3 semiempirical calculations.

MATERIALS AND METHODS

Materials. 5,5-Dimethyl-1-pyrroline-*N*-oxide (DMPO) and 2,2,6,6-tetramethylpiperidine (TEMP) as well as rose bengal (RB), riboflavin, and epigallocatechin gallate (EGCG) were purchased from Sigma, St. Louis, MO. Deionized water for HPLC and EPR experiments (18 MΩ) was obtained from a Milli-Q water purification system (Millipore, Bedford, MA). Methanol for HPLC analysis was of chromatographic grade and purchased from Merck, Darmstadt, Germany. All other chemicals including ethylenediaminetetraacetic acid (EDTA), hydrogen peroxide (H_2O_2), ferrous sulfate ($FeSO_4$), and acetone were made in China and obtained at the highest available purities.

Sample Isolation. The wine grapes (*V. vinifera*, 1 kg) bought in a local fruit store were extracted with 250 mL of acetone for three times, yielding an acetone extract (1.8 g). The acetone extract was then analyzed by HPLC [column, Agilent Extend C18 column, 4.6 × 150 mm i.d., 5 μm; flow rate, 0.8 mL min^{-1}; wavelength, 280 nm; solvent MeOH (B phase)/H_2O (A phase), 30% (B, 0 min)−70% (B, 40 min)] and further separated by preparative-scale HPLC [column, Shimadzu RP Shim-pack PRC ODS, 20 × 250 mm, i.d., 10 μm; flow rate, 8 mL min^{-1}; wavelength, 280 nm; solvent MeOH (B phase)/H_2O (A phase), 28% (B, 0 min)−60% (B, 80 min)] to give resveratrol (0.28%, 28.5 mg), pallidol (0.23%, 22.8 mg), and amurensin G (0.1%, 9.7 mg). The identities of these compounds were confirmed by the fact that increasing peaks were observed when each standard (*17*, *19*) was co-injected with the acetone extract.

EPR Measurements. Hydroxyl radical $^{\bullet}OH$ was formed in a Fenton type reaction ($Fe^{2+} + H_2O_2 \rightarrow Fe^{3+} + {}^{\bullet}OH + OH$) and trapped by DMPO to generate DMPO−OH adducts. The reaction mixtures contained the following reagents at their final concentrations: 25 mM H_2O_2, 250 μM $FeSO_4$, 50 mM purified DMPO, and various concentrations of polyphenols freshly dissolved in acetone. The reactions were stimulated by the last addition of $FeSO_4$ and, immediately, samples were transferred to a quartz capillary. They were then fit into the cavity of a Bruker A300 X-band EPR spectrometer and instantly detected. The conditions of EPR measurements were the same as in the literature (*17*).

Superoxide anion $O_2^{\bullet}$ was generated in the photoirradiated riboflavin/EDTA system. Samples consisted of 0.3 mM riboflavin, 5.0 mM EDTA, 50 mM purified DMPO, and several concentrations of polyphenols in acetone. The mixtures were transferred into a quartz capillary and placed into the EPR cavity. After irradiation by an Hg lamp (power = 100 W) at room temperature for 30 s, EPR spectra were recorded immediately with the UV light on. EPR parameters were set as in the literature (*17*).

Singlet oxygen $^1O_2$ was obtained by photoirradiated RB with air oxygen, and TEMP was a widely used $^1O_2$ trapper. 18 μM RB, 23 mM TEMP, and diverse concentrations of polyphenols were included in the reaction mixtures that were irradiated for 2 min at a distance of 150 cm from the lens of an Hg lamp (power = 100 W). Then EPR spectra were recorded as soon as possible. Scan conditions were the same as in the literature (*17*).

HPLC-ESI-MS^2 Analysis. Samples for HPLC-ESI-MS^2 experiments were composed of 75 μL of 18 μM RB, 75 μL of 23 mM TEMP, and 15 μL of 0.55 mM polyphenols that were freshly dissolved in acetone (only acetone present was the blank control). Then the reaction mixtures were irradiated by a mercury lamp (300 W, $\lambda > 320$ nm, Shanghai Yamin) for 2 min at room temperature. Before irradiation, the UV lamp had been turned on for at least 30 min to reach an equilibrious status. Instantly, 20 μL of the reaction mixture was withdrawn and analyzed by HPLC-ESI-MS^2. HPLC-ESI-MS^2 assays were carried out on an Agilent 1100 system coupled with a Bruker Esquire 3000^{plus} ion trap mass spectrometer (Bruker-Franzen Analytik GmbH, Bremen, Germany). The Agilent 1100 system includes a G1311A QuatPump, a G1322 degasser, a G1314A variable wave detector (VWD), a model 7725i injection valve with a 20 μL loop, and an Agilent ChemStation for LC. The mass spectrometer was equipped with an electrospray ionization (ESI) interface.

Samples were analyzed on an Agilent reversed-phase C8 column (150 mm × 4.6 mm i.d., 5 μm), using an isocratic elution comprising 43% MeOH and 57% water with a flow rate of 0.7 mL min^{-1} at room temperature. Individual chromatograms were recorded at 280 nm, and LC effluent was induced into the ESI source with a T-junction in a splitting ratio of 2:1. Negative ion mode of ESI was performed as it easily provided extensive information. Nitrogen was used as the nebulizing and drying gas at a flow rate of 10 L min^{-1} and a back-pressure of 30 psi. Helium as the collision gas was introduced into the trap with an estimated pressure of 6×10^{-6} mbar. The fragmentation amplitude was set at 1.0 V, and the isolation width of the precursor ion was 2.0 m/z units. The mass scan range was m/z 50−1000 with a speed of 13000 m/z units s^{-1}. Data acquisition was performed using Esquire 5.0 software.

FTICR-MS Analysis. An offline Apex III (7.0 T) Fourier transform ion cyclotron resonance (FTICR) mass spectrometer (Bruker, Billerica, MA) in the negative ESI mode was employed. The needle voltage and the temperature of the drying gas were 4.5 kV and 250 °C, respectively. Nitrogen (N_2) as the drying and nebulizing gas at a pressure of 35 psi and 30 arbitrary units, respectively, was set. Samples and a mobile phase stream including H_2O/CH_3OH (10:90) were infused at a flow rate of 3.0 μL min^{-1}.

PM3 Calculation. Geometry optimization and calculations were accomplished using the Gaussian03 quantum chemistry package. The structures of ground states, transition states, and intermediates were optimized at semiempirical Hartree−Fock PM3 level.

RESULTS

Scavenging Capacities of Resveratrol and Its Oligomers on •OH. •OH was the deoxidized product of H_2O_2 in aqueous solutions and detected as DMPO−OH adducts, which exhibit a well-characterized EPR spectra of 1:2:2:1 pattern with the hyperfine splitting constants $a_N = a^H_B = 14.92$ G (*17*). Compared to the blank control, in which only acetone was present, the addition of resveratrol and its oligomers (> 1.0 mM in acetone) caused only < 30.0% inhibition of DMPO−OH adducts. It is remarkably less effective than those of well-established •OH quenchers such as α-lipoic acid and prion protein (*25*, *26*), indicating that resveratrol and its oligomers are not very effective scavengers on •OH.

Scavenging Capacities of Resveratrol and Its Oligomers on $O_2^{\bullet-}$. $O_2^{\bullet-}$ is known to be produced when the UV light acts on riboflavin in the presence of molecular oxygen. $O_2^{\bullet-}$ was instantly trapped by DMPO and its EPR spectra with the hyperfine splitting constants $a_N = 14.3$ G, $a_\beta^H = 11.7$ G, and $a_\gamma^H = 1.3$ G obtained as in the literature (*17*). Herein, > 1 mM resveratrol (3,4′,5-trihydroxystilbene) and its oligomers attenuated < 70% EPR signal intensities of DMPO/$O_2^{\bullet-}$ adducts, which were much weaker than those of the well-known $O_2^{\bullet-}$ quenchers, for instance, 3,3′,4′,5-tetrahydroxystilbene ($IC_{50} = 2.69$ μM) and 3,3′,4,4′,5,5′-hexahydroxystilbene ($IC_{50} = 5.02$ μM) (*27*), both of which are resveratrol analogues. This demonstrated that these polyphenols are not very potent on scavenging $O_2^{\bullet-}$.

Quenching Capacities of Resveratrol and Its Oligomers on $^1O_2$. $^1O_2$ was generated through a major energy transfer pathway and a minor charge transfer pathway in the photoexcited RB system. $^1O_2$ reacts with TEMP to form TEMP−$^1O_2$ adducts, that is, TEMPO, showing a characteristic EPR spectral pattern of three equal intensity lines ($a^N = 17.2$ G, $g = 2.0056$). **Figure 2** reveals that amurensin G, a naturally occurring resveratrol trimer (**Figure 1**), inhibited the formation of TEMPO in a dose-dependent manner. Only 5.18 μM amurensin G was required to inhibit 50% $^1O_2$ generation, comparable to the case of curcumin, which is a well-known $^1O_2$ quencher ($IC_{50} = 2.75$ μM) (*28*), and the addition of 73.3 μM amurensin G caused complete inhibition.

Besides, using the kinetic model established in our previous work (*17*), rate constants (k_Q) for the reaction of quenchers with $^1O_2$ could be calculated from the slopes ($k_Q/(k_T[TEMP] + k_d)$) when V^{1O2}/V^{TEMP} versus concentrations of quenchers are plotted. Herein k_T is the rate constant for the reaction of TEMP with $^1O_2$, and k_d is the decay rate for $^1O_2$ in water. V^{1O2}/V^{TEMP} represents the ratios of the EPR signal intensities in the absence and presence of quenchers. For example, as shown in **Figure 2**, the slope for amurensin G was observed as 0.2385 ($R^2 = 0.99$), and so its k_Q value was found to be 1.12×10^{10} M^{-1} s^{-1} in the aqueous system. In view of its $IC_{50} = 5.18$ μM, smaller than that of EGCG (14.5 μM), and $k_Q \gg k_T$, it was known that amurensin G was capable of quenching $^1O_2$. In the same way, the IC_{50} and k_Q values of other quenchers were obtained: 18.6 μM and 3.92×10^9 M^{-1} s^{-1} for resveratrol and 5.5 μM and 1.71×10^{10} M^{-1} s^{-1} for pallidol (*17*). Therefore, the conclusion that resveratrol and its oligomers are selective quenchers on $^1O_2$ was reached.

Mechanism Studies for Resveratrol against $^1O_2$ by HPLC-ESI-MS^2. According to the literature (*29*, *30*), the reaction of phenol (PhOH) and $^1O_2$ undergoes an endoperoxide intermediate form to produce 1,4-benzoquinone as the final product. Obviously, the molecular weight of the oxidized product, namely, 1,4-benzoquinone ($M_w = 108$ Da) is 14 Da higher than that of the reaction substrate phenol ($M_w = 94$ Da). We could also assume that resveratrol and its oligomers quench $^1O_2$ via a mechanism similar to that of phenol. Hence, in order to provide convincing evidence of the mechanism, simple reaction systems including RB, TEMP, and polyphenols were conducted in light of the EPR spin-trapping assay for $^1O_2$.

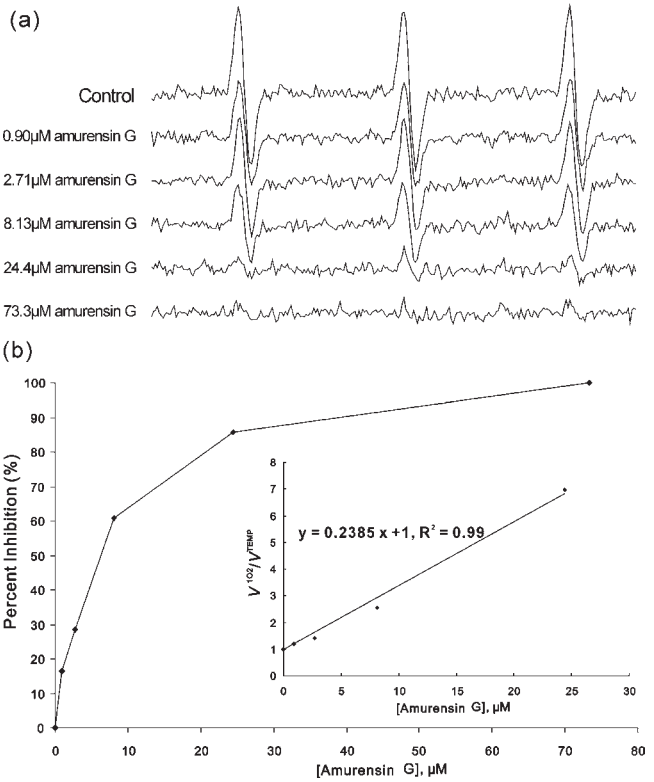

Figure 2. Quenching effects of amurensin G on $^1O_2$. (**a**). Effects of amurensin G on the production of TEMP−$^1O_2$ adducts. Reaction mixtures included 18 μM RB, 23 mM TEMP, and amurensin G at the indicated concentrations, and then they were photoirradiated with a UV lamp for 2 min before instant recording. (**b**) EPR signal intensities of the first peak in **a** were chosen to measure the percent inhibition of amurensin G at different concentrations. (Inset) Plot of V^{1O2}/V^{TEMP} versus concentrations of amurensin G, where V^{1O2}/V^{TEMP} represents the EPR signal intensities in the absence or presence of amurensin G.

Figure 3 (inset) shows the HPLC analysis of the reacted mixture of resveratrol with $^1O_2$, and there are three major peaks designated as 1−3. The peak with the retention time of about 3.2 min represents acetone, which was verified by the injection of acetone alone (data not shown) and disappearance in HPLC-ESI-MS^2 experiments, whereas resveratrol ($C_{14}H_{12}O_3$, $M_w = 228$) as the reactant with $^1O_2$ was almost completely reacted and hardly observed. Concerning its MS^2 spectrum, the neutral losses of C_2H_2O (42 Da), CO_2 (44 Da), and C_3O_2 (68 Da), sequential losses of a C_2H_2O (42 Da) moiety and a CO (28 Da) moiety, and consecutive losses of two C_2H_2O (42 Da) moieties led to the formation of some fragment ions at *m*/*z* 185, 183, 159, 157, and 143. Among them, it has been well elucidated that the fragment C_2H_2O (42 Da) was rather specific for the resorcinol ring in resveratrol (*31*). Then peaks 1, 2, and 3 with molecular weights at 242, 242 and 122, respectively, were newly generated and termed as the products of resveratrol by UV light and/or against $^1O_2$. With respect to peaks 1 and 2 (RQ), HR-FTICR-MS data presented the same and accurate molecular peak at *m*/*z* 241.0498 ($[M - H]^-$), accounting for the elemental composition of $C_{14}H_9O_4$, the theoretical mass of which was 241.0506. It is noteworthy that the molecular weights of **1** and **2** ($M_w = 242$) were 14 Da larger than that of resveratrol ($M_w = 228$). In their MS/MS spectra (**Figure 3**), the precursor ions of 241 ($[M - H]^-$) eliminated 18 Da (H_2O), 28 Da (CO), 44 Da (CO_2), 18 Da (H_2O)

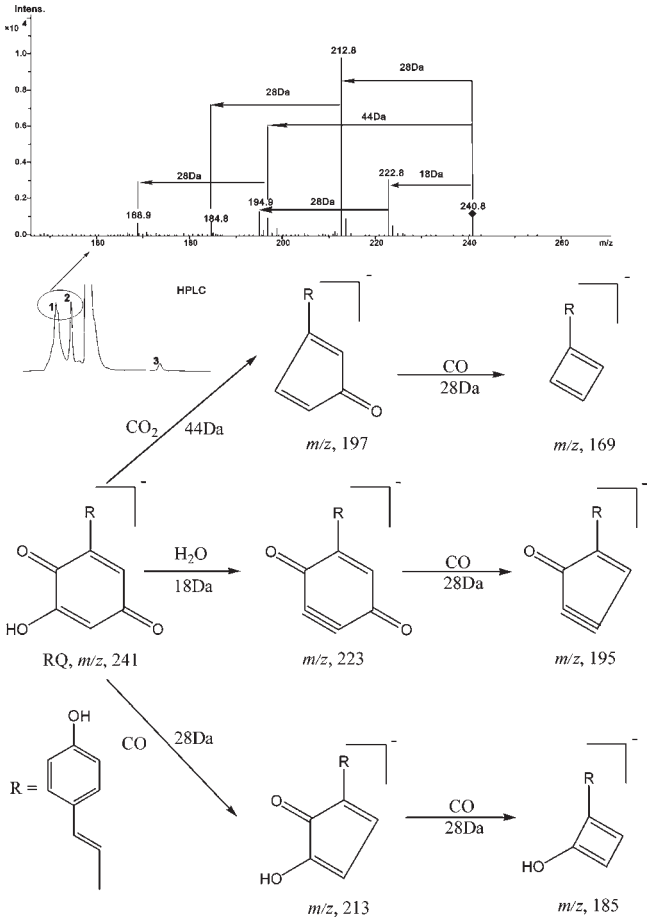

Figure 3. Key fragments observed in the MS/MS spectra of RQ (peaks 1 and 2) at 241 ($[M - H]^-$) and the proposed fragmentation pathways for RQ (peaks 1 and 2). (Inset) HPLC-UV chromatogram for the system modeled from the EPR assay for resveratrol with $^1O_2$. 75 μL of 18 μM RB, 75 μL of 23 mM TEMP, and 15 μL of 0.55 mM resveratrol freshly dissolved in acetone were involved, and the system was photoirradiated by a mercury lamp for 2 min at room temperature. Then 20 μL of the mixture was subjected to the HPLC-ESI-MS^2 analysis.

plus 28 Da (CO), two 28 Da (CO), and 28 Da (CO) plus 44 Da (CO_2) to generate dominant fragment ions at m/z 223, 213, 197, 195, 185, and 169. Apparently, no neutral loss C_2H_2O (42 Da) characteristic of the resorcinol ring was observed in the MS^2 spectra. As a result, on the basis of the literature (*29*, *30*), it could be deduced that the resorcinol ring in resveratrol changed into quinones during the oxidation processes by $^1O_2$.

As shown in **Figure 4**, the first step of the reaction about resveratrol with $^1O_2$ was 1,4-cycloaddition of $^1O_2$ to the resorcinol ring of resveratrol, yielding the endoperoxide intermediate IM-1. Then the subsequent reaction might contain two pathways: one was intramolecular H-abstraction of IM-1 to generate IM-2 (pathway A); the other one was hydrolysis and then consecutive loss of a molecular water to give an unstable hydroperoxide IM-2′ and then also IM-2 (pathway B). The two pathways maintained a competitive but equilibrium state in the reaction processes. Finally, the last step is the formation of resveratrol quinones (RQ) by the intramolecular loss of H_2O in IM-2. Additionally, in the *trans* configuration of resveratrol, there is an ethylene bridge that is highly susceptible to ultraviolet-induced isomerization to produce its *cis* configuration (*19*), so two oxidation products with equal molecular weights but different retention times (**Figure 4**) were received.

Furthermore, the compound corresponding to peak 3 with a much lower molecular weight at 122 Da is 4-hydroxybenzaldehyde, which was confirmed by the easily available standard. The aldehyde compound was generated by the photolysis reaction of resveratrol itself; however, how the compound was obtained is still unclear.

Mechanism Studies for Pallidol and Amurensin G by HPLC-ESI-MS^2. Taking advantage of the proposed mechanism for resveratrol, the oxidation products of pallidol and amurensin G were deduced, also supported by their individual MS (/MS) data. With regard to pallidol (**Figure 1**), two photochemical products were originated: one (M_w = 468) was gained by the attack of $^1O_2$ to one of the symmetrical resorcinol ring; the other one (M_w = 482) was obtained through the attack of $^1O_2$ toward both of the resorcins in pallidol. In addition, amurensin G as an example was investigated in detail. The HPLC-UV chromatogram and total ion chromatogram (TIC) of the reacted system for amurensin G

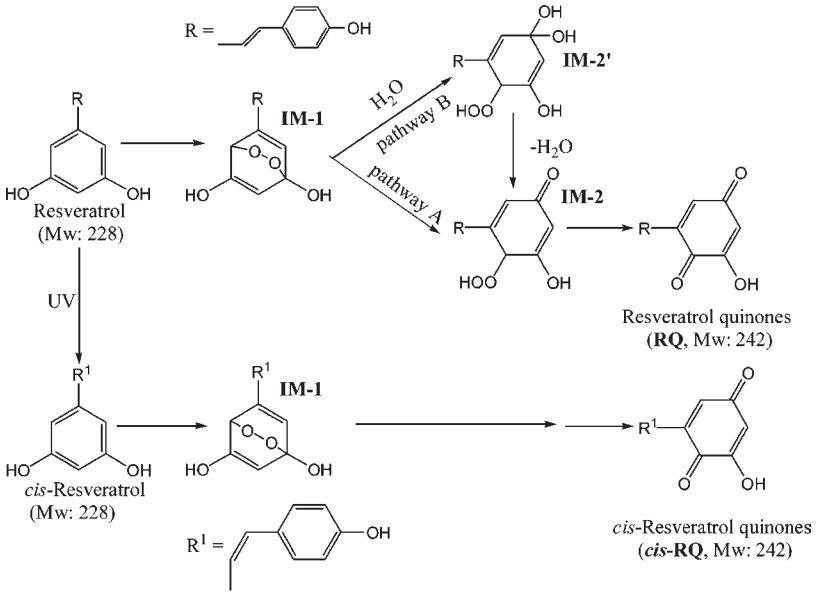

Figure 4. Proposed mechanism for resveratrol against $^1O_2$.

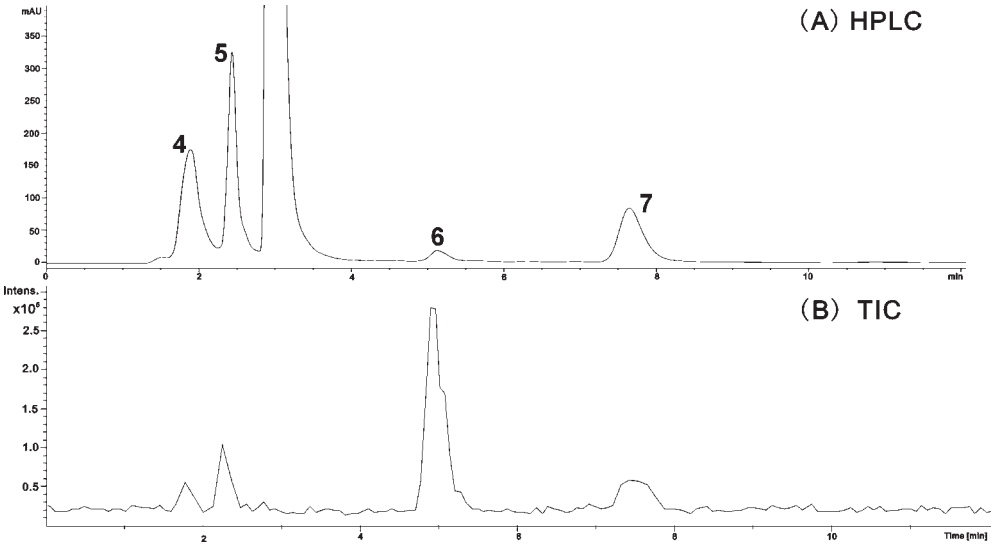

Figure 5. HPLC (**A**) and TIC (**B**) chromatograms of the system stimulated from the EPR assay for amurensin G with $^1O_2$. Sample contained 75 μL of 18 μM RB, 75 μL of 23 mM TEMP, and 15 μL of 0.55 mM amurensin G. After photoirradiation by a mercury lamp for 2 min at room temperature, 20 μL of the reaction mixture was withdrawn and analyzed by HPLC-ESI-MS^2.

are exhibited in **Figure 5**. As C-10a of ring A as well as C-10b and C-14b of ring B has been occupied by different substituents, there were three free reaction sites (11a, 11c, and 13c) left that could be attacked by $^1O_2$ to form quinones. Among them, each of the two sites (11c and 13c) could be reacted with one molecular $^1O_2$ to yield an identical compound. Because of steric hindrance, it would be easier to produce the quinone compound of ring C than that of ring A. Considering their molecular weights are 14 or 28 Da higher than that of amurensin G (M_w = 680), it appeared that peaks 5 and 4 should be assigned as one quinone formed in ring C (AQ-G, M_w = 694) and two quinones formed in both ring A and ring C (DiAQ-G, M_w = 708), respectively, which were supported by their MS^2 spectra.

Compound **5** (AQ-G) gave the $[M - H]^-$ ions at m/z 693. In its dissociation experiments, the precursor ions of m/z 693 produced the neutral losses of H_2O (18 Da), CO (28 Da), CO_2 (44 Da), phenol moiety (94 Da), and 4-methylenecyclohexa-2,5-dienone (106 Da), resulting in series fragment ions at m/z 675, 665, 649, 599, 587, and 567 (*31*). Abundant fragment 124 Da from m/z 693 to m/z 569 or from m/z 599 to m/z 475 was observed and attributed to the neutral loss of 2-hydroxy[1,4]benzoquinone ($C_6H_4O_3$) present in ring C (**Figure 6**). With respect to compound **4**, the $[M - H]^-$ ion at m/z 707 was obtained in its full-scan mass spectrum. Its MS^2 experiment exhibited fragment ions at m/z 689, 679, 663, 613, 601, and 581 owing to the neutral losses of H_2O (18 Da), CO (28 Da), CO_2 (44 Da), phenol moiety (94 Da), and 4-methylenecyclohexa-2,5-dienone (106 Da). Moreover, the dominant fragment 124 Da from m/z 707 to m/z 583 or from m/z 613 to m/z 489 explained the presence of the quinone groups in **4**. 4-Hydroxybenzaldehyde corresponding to peak 6 (M_w = 122) was also derived in the simulated assay for amurensin G by photolysis reaction. It should be noted that 4-hydroxybenzaldehyde was not generated in each case for resveratrol oligomers such as the dimer pallidol, owing to the different chemical structures of these various quenchers.

PM3 Calculation. To quantitatively describe the possibility of the given reaction, theoretical calculations were performed with PM3 semiempirical molecular orbital calculations, and then a potential energy surface as well as the geometrical optimizations of transition states (TS) or products was gained. Here the hypothetical energy profiles for the reaction of resveratrol with $^1O_2$ are presented in **Figure 7**, together with the possible structures on each surface.

With regard to resveratrol, the first step (**Figure 4**) was 1,4-cycloaddition by spanning a possible transition state TS-01 with the Gibbs free energy at 48.3 kcal mol^{-1} and only one negative imaginary frequency of -605.85 cm^{-1}. The step caused the formation of IM-1, the energy of which was calculated to be only 1.97 kcal mol^{-1} above the substrate resveratrol. During the subsequent pathway A process in the second step (**Figure 4**), IM-1 proceeded through a proposed transition state TS-12 (51.5 kcal mol^{-1}) to yield another important intermediate IM-2 (-15.4 kcal mol^{-1}). Otherwise, for pathway B, IM-1 underwent an additional intermediate IM-2′ (-8.84 kcal mol^{-1}) and two extra transition states TS-12′ (41.8 kcal mol^{-1}) and TS-2′2 (21.6 kcal mol^{-1}). Hence, ΔTS-12 (49.5 kcal mol^{-1}, TS-12 − IM-1) > ΔTS-12′ (39.9 kcal mol^{-1}, TS-12′ − IM-1), indicating that pathway B had greater potential to take place. That is, pathway B played a predominant and key role in the second step (*29*). Finally, through the last transition state TS-12 with the calculated energy at 13.7 kcal mol^{-1}, the proposed product, resveratrol quinones (RQ, -76.1 kcal mol^{-1}), were easily generated owing to the low barrier (29.1 kcal mol^{-1}) between IM-2 and TS-23.

As a result, the total reaction energy for the quenching mechanism of resveratrol on $^1O_2$ was -76.1 kcal mol^{-1}, showing this quenching reaction is an overall exothermic species and may be controlled by thermodynamics rather than kinetics. The results also supported that resveratrol exhibits a good activity against $^1O_2$ through an endoperoxide intermediate form and then a hydrolyzed intermediate form in greater proportion to generate its corresponding quinones. Otherwise, theoretical studies become difficult and no longer adaptive for resveratrol oligomers due to their much larger molecular weights ($M_w \geq 454$). However, it is clearly outlined that the mechanism for resveratrol is well applied for the oligomers proved by their specific MS (/MS) data.

DISCUSSION

A large number of pharmacological studies have pointed out that the moderate consumption of red wine could reduce the adverse effects of a high-fat diet in decreasing the incidence of coronary heart disease, which is termed the "French paradox" (*32*−*34*). Polyphenols, especially resveratrol and its

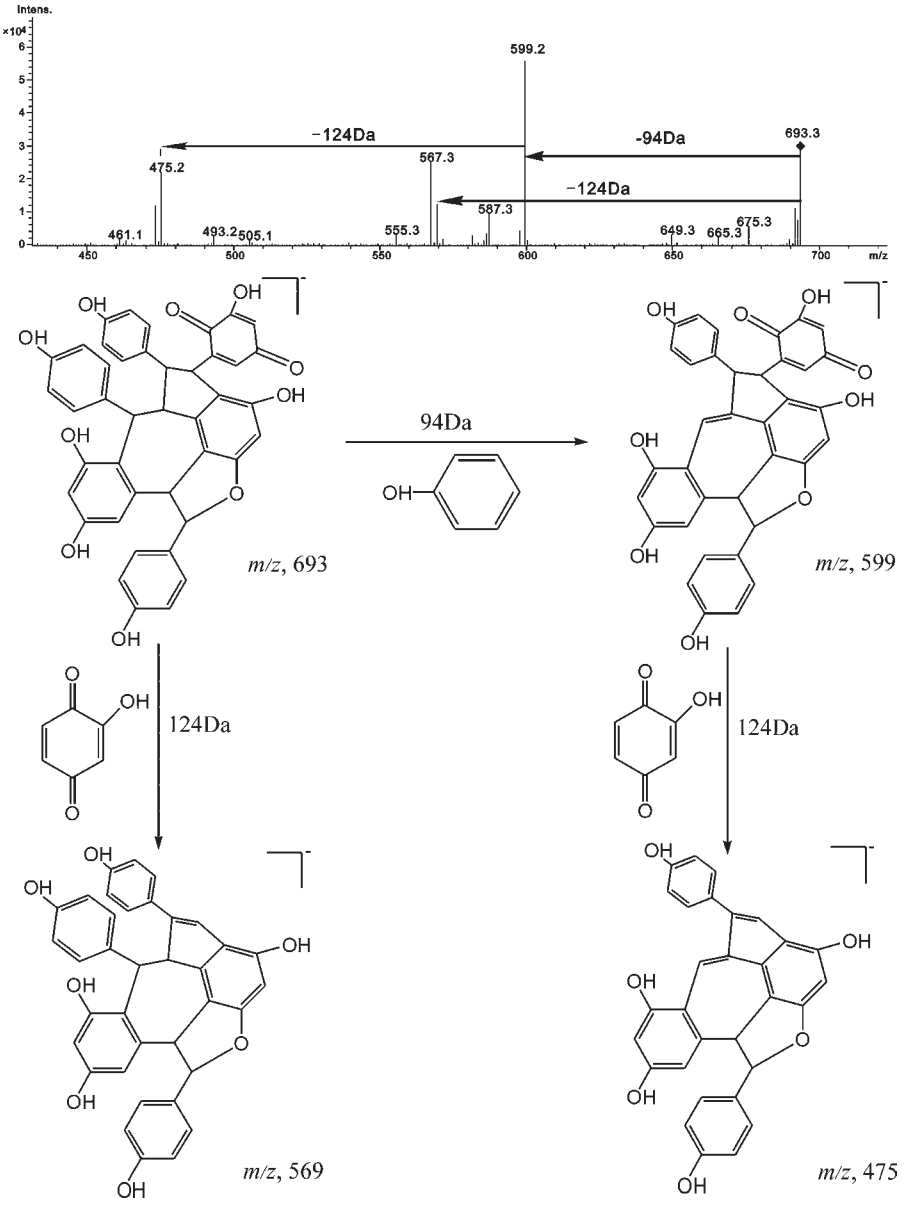

Figure 6. Key fragments observed in the MS/MS spectrum of AQ-G (**5**) at $[M - H]^-$ ion of 693.

oligomers, with powerful antioxidant activities and relatively high contents, were proven to be the main bioactive components responsible for the beneficial effects of red wine (*35*−*38*). Our EPR results demonstrated that resveratrol and its oligomers were selective quenchers on $^1O_2$ at physiological or pharmacological concentrations but not very effective scavengers of $^{\bullet}OH$ and $O_2^{\bullet}$, which were distinctive performances of their antioxidant activities.

Pervious studies (*27*, *39*) have reported that the elimination of $^{\bullet}OH/O_2^{\bullet}$ by phenolic compounds involved three steps: proton transfer from phenolic compounds to $^{\bullet}OH/O_2^{\bullet}$ (initial), rapid scavenging of $^{\bullet}OH/O_2^{\bullet}$ to give H_2O/peroxide and O_2 (second), and oxidation of the phenolic anion by a one- or two-electrons process (ultimate). Obviously, the proton transfer action, namely, the initial step, resulted in the generation of some phenolic free radicals, which could be stabilized by the existence of *o*-hydroxyl groups. That is, these special substitution patterns are necessary for the exceptional antioxidant potencies. When there were no referred substitutions in the molecules of phenolic compounds, no potent scavenging abilities on $^{\bullet}OH/O_2^{\bullet}$ could be gained. For instance, approximately 5 mM resveratrol, the basic unit of the oligomers bearing only resorcinol groups, should be required for 50% inhibition of DMPO/$O_2^{\bullet}$ adducts (*27*). On the other hand, it has been witnessed that an antioxidant might change into a prooxidant accompanied with the generation of some harmful free radicals under special conditions (*40*). Resveratrol as a reducing agent promoted the generation of $^{\bullet}OH$ in the presence of H_2O_2, and Fe(III) ions arose from the oxidation of ferrous ions [Fe(II)] (*41*). These findings could contribute to the weak inhibitory effects of resveratrol and its oligomers on $^{\bullet}OH/O_2^{\bullet}$. Otherwise, to some degree, these polyphenols showed stronger activities against $O_2^{\bullet}$ than $^{\bullet}OH$, because $O_2^{\bullet}$ could easily generate $^1O_2$ (*3*, *42*), and in our work, resveratrol and its oligomers have been reported to be selective quenchers on $^1O_2$.

Assuming that the above scavenging rule is applicable for the cases of resveratrol and its oligomers against $^1O_2$, these polyphenols should not show potent scavenging capacities on $^1O_2$, inconsistent with the obtained results. Therefore, a better understanding of the quenching mechanism of resveratrol and its oligomers on $^1O_2$ is certainly desirable. Thus, a mimetic HPLC-ESI-MS^2 assay was designed in accordance with the EPR assay for $^1O_2$. It is now well established that resveratrol and its

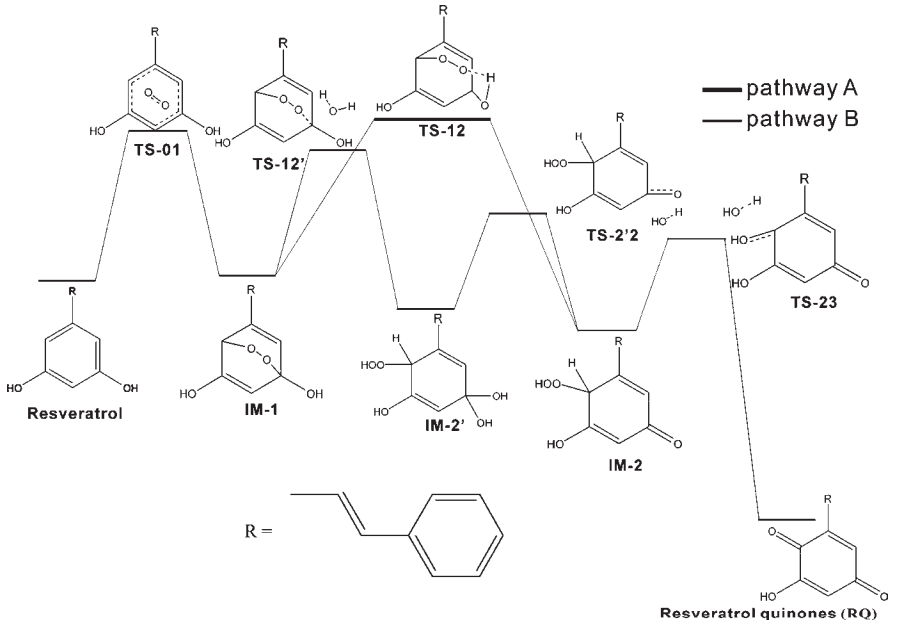

Figure 7. Hypothetical energy profiles for the quenching mechanism of resveratrol on $^1O_2$ using PM3 semiempirical molecular orbital calculations with Gaussian03 quantum chemistry package.

oligomers quench $^1O_2$ in their resorcinol rings, which are valid functional groups.

Interestingly, using the documented mechanism, the quenching activities of pallidol and amurensin G should be twice (IC_{50} to IC_{50}) more effective than that of resveratrol as there are two reaction sites in pallidol and amurensin G while only one in resveratrol. However, actually, they were about 2.95 and 3.58 times stronger, respectively. Perhaps this is a consequence of the participation of both physical and chemical quenching. Quenchers are always regenerated in physical reactions, whereas chemical reactions invariably resulted in the destruction of quenchers and thus in loss of antioxidant protection. It is well recognized (*43*) that the reactions of quenchers with $^1O_2$ may be physical and/or chemical. Sometimes the percentage of physical processes is higher than that of chemical processes. For example, β-carotene quenches $^1O_2$ by a very efficient and dominant electronic energy transfer followed by an intersystem crossing (*44*), whereas both physical and chemical quenchings have been implicated in the mechanism of α-tocopherol against $^1O_2$ (*43*). The balance between these two reactions is sensitively dependent on spin−orbit coupling properties and entropy factors that lie on the critical portions of the reaction coordinates (*43*).

In conclusion, using the HPLC-ESI-MS^2 technique and theoretical studies, the reactions of resveratrol and its oligomers on $^1O_2$ proceeded by physical and chemical quenchings, which is through an endoperoxide intermediate form and then a hydrolyzed intermediate form in greater proportion to generate quinones. Of course, selective activities of resveratrol and its oligomers against $^1O_2$ reveal that they may be drug candidates for treating $^1O_2$-mediated diseases. In addition, through quenching light-dependent ROS, wine grapes, as one of the most popular edible fruits, represent high properties to attenuate the photooxidative stress induced by UV irradiation.

ABBREVIATIONS USED

EPR, electron paramagnetic resonance; ROS, reactive oxygen species; $^{\bullet}OH$, hydroxyl radical; $O_2^{\bullet}$, superoxide anion; $^1O_2$, singlet oxygen; IC_{50}, concentration of quencher required to inhibit 50% $^1O_2$ generation; k_Q, rate constant of the reaction between quencher and $^1O_2$; HPLC-ESI-MS^2, high-performance liquid chromatography−tandem mass spectrometry; HR-FTICR-MS, high-resolution Fourier transform ion cyclotron resonance mass spectrometer; PM3, parametrized method 3; UV, ultraviolet; RB, rose bengal; TIC, total ion chromatogram; RQ, resveratrol quinones generated from the reaction between resveratrol and $^1O_2$; AQ-G and DiAQ-G, quinone products of amurensin G with $^1O_2$; TS, proposed transition states; IM, intermediate; DMPO, 5,5-dimethyl-1-pyrroline-*N*-oxide; TEMP, 2,2,6,6-tetramethylpiperidine.

LITERATURE CITED

(1) Redmond, R. W.; Gamlin, J. N. A compilation of singlet oxygen yields from biologically relevant molecules. *Photochem. Photobiol.* **1999**, *70*, 391–475.

(2) Nakano, M.; Takayama, K.; Shimizu, Y.; Tsuji, Y.; Inaba, H.; Migita, T. Spectroscopic evidence for the generation of singlet oxygen in self-reaction of sec-peroxy radicals. *J. Am. Chem. Soc.* **1976**, *98*, 1974–1975.

(3) Straight, R. C.; Spikes, J. D. Photosensitized oxidation of biomolecules. In *Singlet O_2*, Frimer, A. A, Eds.; CRC Press: Boca Raton, 1985; 4, 91−143.

(4) Hofer, T.; Badouard, C.; Bajak, E.; Ravanat, J. L.; Mattsson, A.; Cotgreave, I. A. Hydrogen peroxide causes greater oxidation in cellular RNA than in DNA. *Biol. Chem.* **2005**, *386*, 333–337.

(5) Davies, M. J. Singlet oxygen-mediated damage to proteins and its consequences. *Biochem. Biophys. Res. Commun.* **2003**, *305*, 761–770.

(6) Foote, C. S. Photosensitized oxidation and singlet oxygen: consequences in biological systems. In *Free Radicals in Biology*; Proyer, W. A, Eds.; Academic Press: New York, 1976; 85−133.

(7) Davies, M. J.; Truscott, R. J. W. Photo-oxidation of protein and its role in cataractogenesis. *J Photochem. Photobiol. B* **2001**, *63*, 114–125.

(8) Tatsushi, T.; Yuko, I. DNA damage induced by coexposure to PAHs and light. *Environ. Toxic. Pharm.* **2007**, *23*, 256–263.

(9) Vitrac, X.; Monti, J. P.; Vercauteren, J.; Deffieux, G.; Mérillon, J. M. Direct liquid chromatographic analysis of resveratrol derivatives and flavanonols in wines with absorbance and fluorescence detection. *Anal. Chim. Acta* **2002**, *458*, 103–110.

(10) Rudnitskaya, A.; Rocha, S. M.; Legin, A.; Pereira, V.; Marques, J. C. Evaluation of the feasibility of the electronic tongue as a rapid analytical tool for wine age prediction and quantification of the organic acids and phenolic compounds. The case-study of Madeira wine. *Anal. Chim. Acta* **2010**, *662*, 82–89.

(11) Jang, M. S.; Cai, L. N.; Udeani, G. O.; Slowing, K. V.; Thomas, C. F.; Beecher, C. W. W; Fong, H. S. H.; Farnsworth, N. R.; Kinghorn, D.; Mehta, R. G.; Moon, R. C.; Pezzuto, J. M. Cancer chemopreventive activity of resveratrol, a natural product derived from grapes. *Science* **1997**, *275*, 218–220.
(12) Lin, J. N.; Lin, V. C. H.; Rau, K. M.; Shieh, P. C.; Kuo, D. H.; Shieh, J. C.; Chen, W. J.; Tsai, S. C.; Way, T. D. Resveratrol modulates tumor cell proliferation and protein translation via SIRT1-dependent AMPK activation. *J. Agric. Food Chem.* **2010**, *58*, 1584–1592.
(13) Soleas, G. J.; Diamandis, E. P.; Goldberg, D. M. Resveratrol: a molecule whose time has come? and gone? *Clin. Biochem.* **1997**, *30*, 91–113.
(14) Lee, S. K.; Zhang, W.; Sanderson, B. J. S. Selective growth inhibition of human leukemia and human lymphoblastoid cells by resveratrol via cell cycle arrest and apoptosis induction. *J. Agric. Food. Chem.* **2008**, *56*, 7572–7577.
(15) Emilia, M. J.; Wenzel, U.; Daniel, H.; Planas, J. M. Resveratrol induces apoptosis through ROS-dependent mitochondria pathway in HT-29 human colorectal carcinoma cells. *J. Agric. Food. Chem.* **2008**, *56*, 4813–4818.
(16) Cichewicz, R. H.; Kouzi, S. A. Resveratrol oligomers: structure, chemistry, and biological activity. In *Studies in Natural Products Chemistry*; Rahman, A. U, Eds., Elsevier Science: B. V., 2002; 26, 506−579.
(17) He, S.; Jiang, L. Y.; Wu, B.; Pan, Y. J.; Sun, C. R. Pallidol, a resveratrol dimer from red wine, is a selective singlet oxygen quencher. *Biochem. Biophys. Res. Commun.* **2008**, *379*, 283–287.
(18) He, S.; Jiang, L. Y.; Wu, B.; Pan, Y. J.; Sun, C. R. Two novel antioxidative stilbene tetramers from *Parthenocissus laetevirens*. *Helv. Chim. Acta* **2009**, *92*, 1260–1267.
(19) He, S.; Jiang, L. Y.; Wu, B.; Li, C.; Pan., Y. J. Chunganenol: an unusual antioxidative resveratrol hexamer from *Vitis chunganensis*. *J. Org. Chem.* **2009**, *74*, 7966–7969.
(20) Kondo, K.; Kurihara, M.; Miyata, N.; Suzuki., T.; Toyoda., M. Scavenging mechanisms of (-)-epigallocatechin gallate and (-)-epicatechin gallate on peroxyl radicals and formation of superoxide during the inhibitory action. *Free. Radic. Bio. Med.* **1999**, *27*, 855–863.
(21) Amarante, G. W.; Milagre, H. M. S.; Vaz, B. G.; Ferreira, B. R.V.; Eberlin, M. N.; Coelho, F. Dualistic nature of the mechanism of the morita-baylis-hillman reaction probed by electrospray ionization mass spectrometry. *J. Org. Chem.* **2009**, *74*, 3031–3037.
(22) Zhang, H. Y.; Sun, Y. M.; Wang, X. L. Substituent effects on O-H bond dissociation enthalpies and ionization potentials of catechols: a DFT study and its implications in the rational design of phenolic antioxidants and elucidation of structure-activity relationships for flavonoid antioxidants. *Chem. Eur. J.* **2003**, *9*, 502–508.
(23) Prouillac, C.; Vicendo, P.; Garrigues, J. C.; Poteau, R.; Rima, G. Evaluation of new thiadiazoles and benzothiazoles as potential radioprotectors: free radical scavenging activity in vitro and theoretical studies (QSAR, DFT). *Free Radic. Bio. Med.* **2009**, *46*, 1139–1148.
(24) Rossi, M.; Caruso, F.; Opazo, C.; Salciccioli, J. Crystal and molecular structure of piceatannol; scavenging features of resveratrol and piceatannol on hydroxyl and peroxyl radicals and docking with transthyretin. *J. Agric. Food. Chem.* **2008**, *56*, 10557–10566.
(25) Matsugo, S.; Yan, L. J.; Han, D.; Trischler, H. J.; Packer, L. Elucidation of antioxidant activity of α-lipoic acid toward hydroxyl radical. *Biochem. Biophys. Res. Commun.* **1995**, *208*, 161–167.
(26) Nadal, R. C.; Abdelraheim, S. R.; Brazier, M. W.; Rigby, S. E. J.; Brown, D. R.; Viles, J. H. Prion protein does not rodox-silence Cu^{2+}, but is a sacrificial quencher of hydroxyl radicals. *Free Radic. Biol. Med.* **2007**, *42*, 79–89.
(27) Marek, M.; Walter, J.; Norbert, H.; Thomas, E.; Zsuzsanna, H.; Thomas, S.; Hans, N.; Lars, G. Antioxidant, prooxidant and cytotoxic activity of hydroxylated resveratrol analogues: structure−activity relationship. *Biochem. Pharmacol.* **2005**, *69*, 903–912.
(28) Das, K. C.; Das, C. K. Curcumin (diferuloylmethane), a singlet oxygen ($^1O_2$) quencher. *Biochem. Biophys. Res. Commun.* **2002**, *295*, 62–66.
(29) Li, C.; Hoffman, M. Z. Oxidation of phenol by singlet oxygen photosensitized by the tris (2, 2′-bipyridine) ruthenium (II) ion. *J. Phys. Chem. A* **2000**, *104*, 5998–6002.
(30) Briviba, K.; Devasagayam, T. P. A.; Sies, H.; Steenken, S. Selective para hydroxylation of phenol and aniline by singlet molecular oxygen. *Chem. Res. Toxicol.* **1993**, *6*, 548–553.
(31) Chen, J. J.; He, S.; Mao, H.; Sun, C. R.; Pan, Y. J. Characterization of polyphenol compounds from the roots and stems of *Parthenocissus laetevirens* by high-performance liquid chromatography/tandem mass spectrometry. *Rapid Commun. Mass Spectrom.* **2009**, *23*, 737–744.
(32) Renaud, S.; Logeril, M. D. Wine, alcohol, platelets, and the French paradox for coronary heart disease. *Lancet* **1992**, *339*, 1523–1526.
(33) Goldberg, D. M.; Hahn, S. E.; Parkes, J. G. Beyond alcohol: beverage consumption and cardiovascular mortality. *Clin. Chim. Acta* **1995**, *237*, 155–187.
(34) Iriti, M.; Faoro, F. Bioactivity of grape chemicals for human health. *Nat. Prod. Commun.* **2009**, *4*, 611–634.
(35) Frankel, E. N.; Kanner, J.; German, J. B.; Parks, E.; Kinsella, J. E. Inhibition of human low density lipoprotein by phenolic substances in red wine. *Lancet* **1993**, *341*, 454–457.
(36) Kanner, J.; Frankel, E.; Granit, R.; German, B.; Kinsella, J. E. Natural antioxidants in grapes and wines. *J. Agric. Food Chem.* **1994**, *42*, 64–69.
(37) Frankel, E. N.; Waterhouse, A.; Teissedre, P. Principal phenolic phytochemicals in selected California wines and their antioxidant activity in inhibiting oxidation of low-density lipoproteins. *J. Agric. Food Chem.* **1995**, *43*, 890–894.
(38) Pezzuto, J. M. Grapes and human health: a perspective. *J. Agric. Food. Chem.* **2008**, *56*, 6777–6784.
(39) Nanni, E. J.; Stallings, M. D.; Sawyer, D. T. Does superoxide ion oxidize catechol, α-tocopherol, and ascorbic acid by direct electron transfer? *J. Am. Chem. Soc.* **1980**, *102*, 4481–4485.
(40) Bowry, V. W.; Stocker, R. Tocopherol-mediated peroxiation. the prooxidation effect of vitamin E on the radical-initiated oxidation of human low-density lipoprotein. *J. Am. Chem. Soc.* **1993**, *115*, 6029–6044.
(41) Zheng, L. F.; Wei, Q. Y.; Cai, Y. J.; Fang, J. G.; Zhou, B.; Yang, L.; Liu, Z. L. DNA damage induced by resveratrol and its synthetic analogues in the presence of Cu (II) ions: mechanism and structure-activity relationship. *Free Radic. Biol. Med.* **2006**, *41*, 1807–1816.
(42) Halliwell, B. Superoxide dismutase, catalase and glutathione peroxidase: solutions to the problems of living with oxygen. *New Phytol.* **1974**, *73*, 1075–1086.
(43) Gorman, A. A.; Gould, I. R.; Hamblett, I.; Standen, M. C. Reversible exciplex formation between singlet oxygen, $^1\Delta_g$, and vitamin E. solvent and temperature effects. *J. Am. Chem. Soc.* **1984**, *106*, 6956–6959.
(44) Farmilo, A.; Wilkinson, F. On the mechanism of quenching of singlet oxygen in solution. *Photochem. Photobiol.* **1973**, *18*, 447–450.

Received for review May 25, 2010. Revised manuscript received July 16, 2010. Accepted July 17, 2010. We gratefully acknowledge financial support from NSFC (20772109) and NCET-06-520.